Journal of Pharmacological and Toxicological Methods 96 (2019) 15–26

Contents lists available at ScienceDirect

Journal of Pharmacological and Toxicological Methods

journal homepage: www.elsevier.com/locate/jpharmtox

Research article

Impact of disease state on arrhythmic event detection by action potential modelling in cardiac safety pharmacology

Bernard Christophe[a,*], William J. Crumb Jr[b]

[a] Scaptest, rue d'albroux, 10, B-1367 Grand Rosière Hottomont, Belgium
[b] Nova Research Laboratories LLC, 1441 Canal Street, New Orleans, LA 70112, USA

ARTICLE INFO

Keywords:
CiPA initiative
Congestive heart failure
Drug screening
Early afterdepolarization
Human ventricular myocyte
IC_{50s}-V_{min} metric
in silico cardiac action potential simulation
Proarrhythmic liability prediction
Safety pharmacology
Hypertrophic cardiomyopathy

ABSTRACT

Introduction: The use of *in silico* cardiac action potential simulations is one of the pillars of the CiPA initiative (Comprehensive *in vitro* Proarrhythmia Assay) currently under evaluation designed to detect more accurately proarrhythmic liabilities of new drug candidate. In order to take into account the variability of clinical situations, we propose to improve this method by studying the impact of various disease states on arrhythmic events induced by 30 torsadogenic or non-torsadogenic compounds.

Method: In silico modelling was done on the human myocytes using the Dutta revised O'Hara-Rudy algorithm. Results were analysed using a new metric based on the compound IC_{50s} against the seven cardiac ionic currents considered to be the most important by the CiPA initiative (I_{Kr}, I_{Ks}, I_{Na}, I_{NaL}, I_{K1}, I_{to}, I_{CaL}) and the minimal rate of action potential voltage decrease calculated at the early-afterdepolarization (EAD) take-off membrane voltage (V_{min}).

Results: The specific threshold at which each torsadogenic compounds induced EAD, was exacerbated by the presence of cardiac risk factors ranked as follows: congestive heart failure > hypertrophic cardiomyopathy > cardiac pause > no risk factor. Non-torsadogenic compounds induced no EAD even in the presence of cardiac risk factors.

Discussion: The present study highlighted the impact of pre-existing cardiovascular disease on arrhythmic event detection suggesting that disease state modelling may need to be incorporated in order to fully realize the goal of the CiPA paradigm in a more accurate predictability of proarrhythmic liabilities of new drug candidate.

1. Introduction

The Comprehensive *in vitro* Proarrhythmia Assay (CiPA) initiative (Sager, Gintant, Turner, Petit, & Stockbridge, 2014) is a new approach currently under evaluation (Cavero & Holzgrefe, 2014, 2015; Fermini et al., 2015; Kleiman, Shah, & Morganroth, 2014; Mason, 2017) designed to detect more accurately proarrhthymic liabilities of new drug candidates and support crucial decision-making process early in cardiac safety pharmacology. This initiative is still to be approved by clinicians in drug development and by regulatory authorities. Based on the increasing confidence placed in computational simulations during the last decade, especially for drug safety assessment (Mirams & Noble, 2011; Passini et al., 2017) one component of the CiPA initiative is to evaluate the putative effects of drugs on healthy human cardiac action potential (AP) by *in silico* modelling. However, the intent of this series of assays is to not simply predict drug-associated QTc interval prolongation but also to predict the likelihood of proarrhythmic events (Crumb, Christophe, & Shah, 2017). It is well known that in general, the incidence of drug-associated torsade de pointes (TdP) is often extremely low (Darpo, 2010; Sarganas et al., 2014) but it can also be also

Abbreviations: AP, action potential; APA, action potential amplitude; $APD_{40,\ 60\ or\ 90}$, action potential duration at 40, 60 or 90% of APA repolarization; CHF, congestive heart failure; CiPA, comprehensive *in vitro* proarrhythmia assay; C_{max}, maximal free plasma concentration; CL, cycle length; HCM, hypertrophic cardiomyopathy; IC_{50}, concentration of a compound inducing 50% of inhibition of a cardiac ionic current activity; IC index, inhibition index calculated from the I_{Kr}, I_{CaL} and I_{NaL} IC_{50s} determined for a compound; EAD, early afterdepolarization; $EFTPC_{max}$, maximal effective free therapeutic concentration; LQT1, 2 or 3, long QT syndrome of type 1, 2 or 3; mM, millimolar; ms, milliseconds; V/s, volts per second; mV, millivolts; ORd, O'Hara-Rudy dynamic model; $T_{90–40}$ and $T_{90–60}$, triangulation estimation (APD_{90}-APD_{40}, APD_{90}-APD_{60}); qnet, net charge carried by six major cardiac currents (I_{Kr}, I_{CaL}, I_{NaL}, I_{to}, I_{Ks}, and I_{K1}) over an entire beat; TdP, torsade de pointes; V_{max}, maximal rate of AP rise; V_{min}, minimal rate of AP voltage decrease at EAD take-off membrane voltage; WP classification, Wisniowska & Polak classification

* Corresponding author.
E-mail addresses: bchristophe@scaptest.com (B. Christophe), w.crumb@novreslab.com (W.J. Crumb).

https://doi.org/10.1016/j.vascn.2018.12.004
Received 1 August 2018; Received in revised form 11 December 2018; Accepted 17 December 2018
Available online 21 December 2018

relatively high (*e.g.* 1.5–9%) for certain drugs such as quinidine (Kay, Plumb, Arciniegas, Henthorn, & Waldo, 1983). Interestingly, many of the drugs with higher incidences of TdP are cardiovascular drugs such as dofetilide, flecainide, sotalol, quinidine for example (Tisdale, 2016). One common feature underlying this increased risk of TdP with these drugs is a patient population with pre-existing arrhythmogenic risk factors. Therefore, to properly evaluate the risk of drug-associated TdP using *in silico* modelling, one should characterize this risk not only under healthy conditions where the incidence is likely low but also under conditions likely to exist in those patients who are at higher risk of drug-associated TdP. The goal of this study was first to explore, using *in silico* action potential modelling, the influence of various underlying cardiac risk factors (Woosley, Heise, Gallo, et al., 2018) such as ischemia, hypokalemia, bradycardia, long QT syndrome of type 1, 2 or 3 (LQT1, LQT2, LQT3), cardiac pause, hypertrophic cardiomyopathy (HCM) and congestive heart failure (CHF) on the incidence of proarrhythmic events (*e.g.* early afterdepolarizations, EAD). In order to predict torsadogenic risk of a compound, various *in silico* parameters have been proposed as metrics including AP duration prolongation (Mirams et al., 2011, 2014), repolarization abnormalities occurrence such as early after depolarization (Christophe, 2013, McMillan et al., 2017, Passini et al., 2017), transmural dispersion of repolarization increase (Christophe, 2015) or the net charge (qnet) carried by six major cardiac currents (I_{Kr}, I_{CaL}, I_{NaL}, I_{to}, I_{Ks}, and I_{K1}) over an entire beat (Chang et al., 2017; Dutta, Chang, et al., 2017). In order to improve the quantification of this torsadogenic risk of a compound, this study proposed a new simple quantitative and predictive metric based upon the relationship existing between an IC index calculated from the potency ratio of a compound to inhibit inward and outward cardiac currents and the minimal rate of AP voltage decrease calculated at the EAD take-off membrane voltage (V_{min}). Finally, the effects of 30 clinical compounds characterized for their inhibitory activity against the seven cardiac ionic currents considered to be the most important by the CiPA initiative (I_{Kr}, I_{Ks}, I_{Na}, I_{NaL}, I_{K1}, I_{to}, I_{CaL}) (Crumb, Vicente, Johannesen, & Strauss, 2016) were analysed under non-failing conditions as well as conditions of cardiac risk factors such cardiac pause, HCM and CHF in order to determine the impact of disease state on arrhythmic event detection during drug preclinical cardiac safety pharmacological studies.

2. Materials and methods

In silico AP modelling of the human epi, mid or endocardial myocyte under non-failing conditions was done using the ORd algorithm fully described by O'Hara et al. (2011, see also the research section of their website: http://rudylab.wustl.edu). For non-failing experimental conditions, equations, constants (extracellular Na^+, K^+ and Ca^{++} ionic concentrations, cell geometry, current conductances) and initial conditions for state variables were used as described in the ORd algorithm. However, the I_{CaL}, I_{NaL}, I_{Kr}, I_{Ks} and I_{K1} conductances were revised according to Dutta, Strauss, Colatsky, and Li (2016) in order to optimize the model for proarrhythmia risk assessment. Simulations were carried out at equilibrium (estimated after 100 beats) under cycle lengths (CL) from 800 to 3000 ms. The effects induced on the AP by the inhibition of three cardiac ionic currents (I_{Kr}, I_{CaL} and I_{NaL}) were tested on the human ventricular endocardial myocytes under a CL of 1000 ms using the Dutta revised ORd algorithm. Eight cardiac risk factors (2 s pause, HCM, CHF, LQT1, LQT2, LQT3, hypokalemia and ischemia) were tested in order to observe their influence on the incidence of proarrhythmic events on the AP obtained by *in silico* simulation of the human ventricular endocardial myocytes under a CL of 1000 ms using the Dutta revised ORd algorithm modified as described in Table 1. Cardiac pause conditions were tested using the Dutta revised ORd algorithm after 103 beats with a 2-seconds pause without stimulation at beats 101 and 102. CHF and HCM conditions were tested using the Dutta revised ORd algorithm modified according to Trenor et al. (2012) and Passini et al. (2016), respectively. Four min ischemia conditions were tested using the Dutta revised ORd algorithm modified according to Rodriguez, Trayanova, and Noble (2006) and Gemmell, Burrage, Rodriguez, and Quinn (2016). LQT1, LQT2 or LQT3 conditions (the three most frequent LQT syndromes, see Misuzawa et al., 2014 for review) were tested using the Dutta revised ORd algorithm with a 100% decrease of G_{Ks}, a 50% decrease of G_{Kr} or a 10-fold increase of the G_{NaL}, respectively. Finally, hypokalemia conditions were tested using the Dutta revised ORd algorithm with decrease of $[K^+]_o$ up to 3.5 mM.

The simulated AP was described by using the following parameters: resting membrane potential (RMP) expressed as millivolts (mV), maximal amplitude of the AP (APA) expressed as mV, maximal rate of AP rise (V_{max}) expressed as volts per second (V/s), duration of the AP measured at 40, 60 or 90% of APA repolarization ($APD_{40,\ 60\ or\ 90}$) expressed as milliseconds (ms), AP triangulation estimations which were calculated as the difference between APD_{90} and APD_{40} or APD_{60} ($T_{90–40}$ or $T_{90–60}$) expressed as ms. As the AP voltage at which an EAD was observed (EAD take-off voltage) was always observed in a stable and restricted range of membrane voltage in the absence or presence of proarrhythmic conditions (-20.8 ± 2.1 mV, $n = 8$; mean ± standard deviation), a new AP parameter (V_{min}, minimal rate of AP voltage decrease at the EAD take-off membrane voltage) was introduced in order to describe the condition under which an EAD was observed. At this point, V_{min} was always equal to zero as voltage decrease moved to voltage increase. In absence of EAD, V_{min} was determined within this range of EAD take-off voltage.

Among the various tested experimental conditions, four were selected in order to test the effects of 30 compounds on EAD occurrence: non-failing conditions as control conditions, 2 s pause as example of slight proarrhythmic risk conditions and finally HCM and CHF as examples of severe proarrhythmic risk conditions. Using manual whole cell patch clamp technique on human expression systems, these 30 compounds were evaluated by Crumb et al. (2016) for their inhibitory activity against the seven cardiac ionic currents (I_{Kr}, I_{Ks}, I_{Na}, I_{to}, I_{K1}, I_{NaL} or I_{CaL}) selected as important by the CiPA Ion Channel Working Group. The great advantage of this data set was not only the large number of compounds studied exclusively using the human systems but also the well-balanced distribution of these compounds with regard to their TdP risk classification. Regarding compounds torsadogenicity, many classifications were proposed and we referred to the Wisniowska & Polak (WP) classification (2017) because they reviewed and summarized all the previously proposed classifications including Crediblemeds (Woosley, Heise, and Romero, 2018) or CiPA (Fermini et al., 2015) classifications for example. According to the WP classification, 8, 15, 4 and 3 of the 30 studied compounds can be categorized as class 1 (compounds classified as TdP positive), class 2 (compounds with contradicting classification, both TdP positive or negative depending of the studies), class 3 (compounds classified as TdP negative) or class 4 (compounds not reported), respectively. The effect of compounds was tested by shifting the conductance of each of the seven currents as described by Mirams et al. (2011) by a scaling factor ranked from 1 (no inhibition) to 0 (full inhibition) which is a function of a multiple (1-fold, 3-fold, 10-fold, 30-fold or 100-fold) of the maximal effective free therapeutic plasma concentration ($EFTPC_{max}$) of the compounds and the IC_{50s} of the compounds for each ionic current (raw data from Crumb et al., 2016). When an EAD was observed, the first multiple inducing an EAD was determined. For each compound concentration, an IC index was calculated as the ratio of the potency of this compound to inhibit at this concentration the most important inward and outward cardiac currents as follows: IC index = (AFKr/((AFNaL + AFCaL)/2))*100 where AFKr, AFNaL and AFCaL represent the active fraction (expressed as percentage) of the I_{Kr}, I_{NaL} and I_{CaL} currents, respectively. An IC index < 100 indicated a higher effect on outward currents (IC index of zero indicated a complete outward inhibition). Conversely, an IC index > 100 indicated a higher effect on inward currents.

Table 1
Description of the changes applied to the Dutta revised ORd algorithm (using human ventricular endocardial myocytes under various experimental conditions and a cycle length of 1000 ms) and description of the effects induced by these changes on the AP parameters.

	2 s pause	HCM	CHF	LQT1	LQT2	LQT3	Hypo kalemia	Ischemia 4 min
Reference		(a)	(b)					(c) (d)
Changes:								
G_{Ks}		−45%		−100%				
G_{Kr}		−45%			−50%			
G_{K1}		−30%	−32%					
G_{Na}								−10%
G_{NaL}		+165%	+200%			x 10-fold		
G_{ncx}		+30%	+175%					
G_{to}		−70%	−60%					
P_{Ca}		+40%						−10%
P_{Cab}			+153%					
P_{Nab}		+165%	−100%					
P_{NaK}		−30%	−10%					
J_{leak}			+500%					
J_{rel}		−20%						
J_{up}		−25%	−50%					
τ_{NaL}			+200%					
τI_{CaLf}		+35%						
τI_{CaLs}		+20%						
$[K^+]_o$							3.5 mM	8 mM
[MgATP]								−12.8%
[MgADP]								x 2.64-fold
[TRPN]		−50%						
Cell volume		+90%						
Results (%)								
RMP	0.0	−0.4	−0.7	0.0	0.0	0.0	+13.1	−11.9
APA	+0.1	+5.7	−1.1	0.0	+0.4	+7.7	+8.2	−11.9
Vmax	+1.8	−0.1	−6.6	+0.1	+1.9	−2.9	−52.1	−67.6
APD_{40}	+6.5	+80.6	+80.1	+12.2	+32.6	+88.1	+19.7	−14.9
APD_{60}	+6.6	+96.5	+96.4	+12.6	+39.1	+109.0	+21.2	−15.5
APD_{90}	+5.1	+98.4	+91.0	+10.7	+40.3	+100.7	+18.4	−15.7
$T_{90–40}$	+1.4	+146.3	+120.4	+6.5	+61.0	+134.4	+14.8	−17.8
$T_{90–60}$	−3.5	+109.3	+59.0	−0.9	+47.3	+51.4	+1.7	−16.8
V_{min}	+3.3	+63.8	+62.6	+8.2	+45.6	+67.7	+18.6	−16.9

(a) Passini et al., 2016; (b) Trenor et al., 2012; (c) Rodriguez et al., 2006; (d) Gemmell et al., 2016; G_{Ks}, slow delayed rectifier K^+ current conductance; G_{Kr}, rapid delayed rectifier K^+ current conductance; G_{K1}, inward rectifier K^+ current conductance; G_{Na}, fast sodium current conductance; G_{NaL}, late Na^+ current conductance; G_{ncx}, Na^+/Ca^{++} exchanger current conductance; G_{to}, transient outward K^+ current conductance; P_{Ca}, Ca^{++} current through the L-type Ca^{++} channel conductance; P_{Cab}, Ca^{++} background current conductance; P_{Nab}, Na^+ background current conductance; P_{NaK}, Na^+/K^+ ATP_{ase} current conductance; J_{leak}, leak Ca^{++} flux; J_{rel}, total Ca^{++} release *via* ryanodine receptors from junctional sarcoplasmic reticulum compartment to myoplasm; J_{up}, total Ca^{++} uptake *via* SERCA(=sarco/endoplasmic reticulum Ca^{++}-ATP_{ase}) pump from myoplasm to network sarcoplasmic reticulum compartment; τ_{NaL}, time of inactivation of I_{NaL}; τI_{CaLf}, time of fast inactivation of I_{CaL}, τI_{CaLs}, time of slow inactivation of I_{CaL}; [MgATP], Mg adenosine triphosphate concentration; [MgADP], Mg adenosine diphosphate concentration; [TRPN], Troponin Ca++ buffer concentration. Results are expressed as percentage of the values observed with the Dutta revised ORd algorithm under non-failing experimental conditions.

3. Results

3.1. EAD occurrence under non-failing and failing experimental conditions

AP obtained by *in silico* simulation of the human ventricular endocardial myocyte using the Dutta revised ORd algorithm under non-failing conditions at a CL of 1000 ms was described by the following parameters: RMP of −88 mV, APA of 128 mV, V_{max} of 255 V/s, APD_{40} of 194 ms, APD_{60} of 228 ms, APD_{90} of 266 ms, $T_{90–40}$ of 72 ms, $T_{90–60}$ of 38 ms (Fig. 1A). An increasing level of I_{Kr} inhibition gradually increased $APD_{40,\ 60\ and\ 90}$ and $T_{90–40}$ and $T_{90–60}$ (Fig. 1A). At 97% I_{Kr} inhibition, EAD was observed at a take-off membrane voltage of −22.0 mV (Fig. 1A). At this EAD take-off membrane voltage, the minimal rate of AP voltage (V_{min} of −0.759 V/s in absence of any I_{Kr} inhibition) tended towards zero and became positive with EAD observed at an I_{Kr} inhibition of 97% (Fig. 1B).

Using the Dutta revised ORd algorithm, the EAD take-off membrane voltage was calculated to be −22.2 and −22.9 mV from the AP obtained by *in silico* simulation of the healthy human ventricular endocardial or midmyocardial myocytes under a CL of 1000 ms, respectively. Due to the absence of EAD on the healthy human ventricular epicardial myocytes (Fig. 2A), this EAD take-off membrane voltage was estimated to be −22.0 mV. In the absence of any I_{Kr} inhibition, V_{min} was calculated to be −1.056, −0.759 or −0.563 V/s for epicardial, endocardial or midmyocardial myocytes, respectively (Fig. 2A). With an increasing level of I_{Kr} inhibition, V_{min} tended towards zero and became positive with EAD observed in endocardial and midmyocardial myocytes at an I_{Kr} inhibition of 97 and 73%, respectively (Fig. 2A). No EAD was observed in epicardial myocyte even with a 100% I_{Kr} inhibition (Fig. 2A).

In the absence of any I_{Kr} inhibition, V_{min} was calculated to be −0.767, −0.759, −0.739 or −0.733 V/s (at an EAD take-off membrane voltage of −20.1, −22.2, −22.0, −22.2 mV) from the AP obtained by *in silico* simulation of the human ventricular endocardial myocytes under a CL of 800, 1000, 2000 or 3000 ms using the Dutta revised ORd algorithm, respectively (Fig. 2B). Again, with an increasing level of I_{Kr} inhibition, V_{min} tended towards zero and became positive with EAD observed at an I_{Kr} inhibition of 100, 97, 93 and 91% at a CL of 800, 1000, 2000 or 3000 ms, respectively.

Using *in silico* simulation of the human ventricular endocardial myocytes under a CL of 1000 ms, increasing I_{Kr} inhibition induced a V_{min} increase up to zero (observed at 97% I_{Kr} inhibition) with a leftward

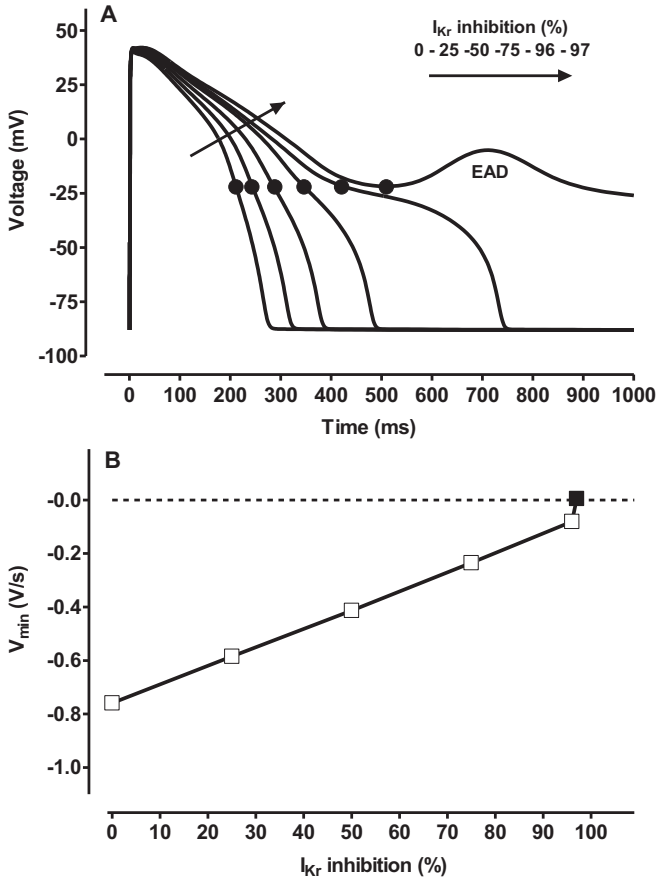

Fig. 1. (A) APs obtained by *in silico* simulation of the human ventricular endocardial myocytes using the Dutta revised ORd algorithm with a cycle length of 1000 ms in the presence of various levels of I_{Kr} inhibition. The ordinate is the membrane voltage (Vm) expressed as millivolts (mV). The abscissa is the time expressed as milliseconds (ms). Closed circles represent the EAD take-off voltage at which V_{min} was determined for each AP (see methods). (B) V_{min} values calculated from these APs. The ordinate is the minimal rate of membrane voltage decrease measured at the EAD take-off voltage (V_{min}) expressed as volts per second (V/s). The abscissa is the percentage of I_{Kr} inhibition. Open and closed squares represent the absence or presence of EAD. Dotted line represents EAD threshold.

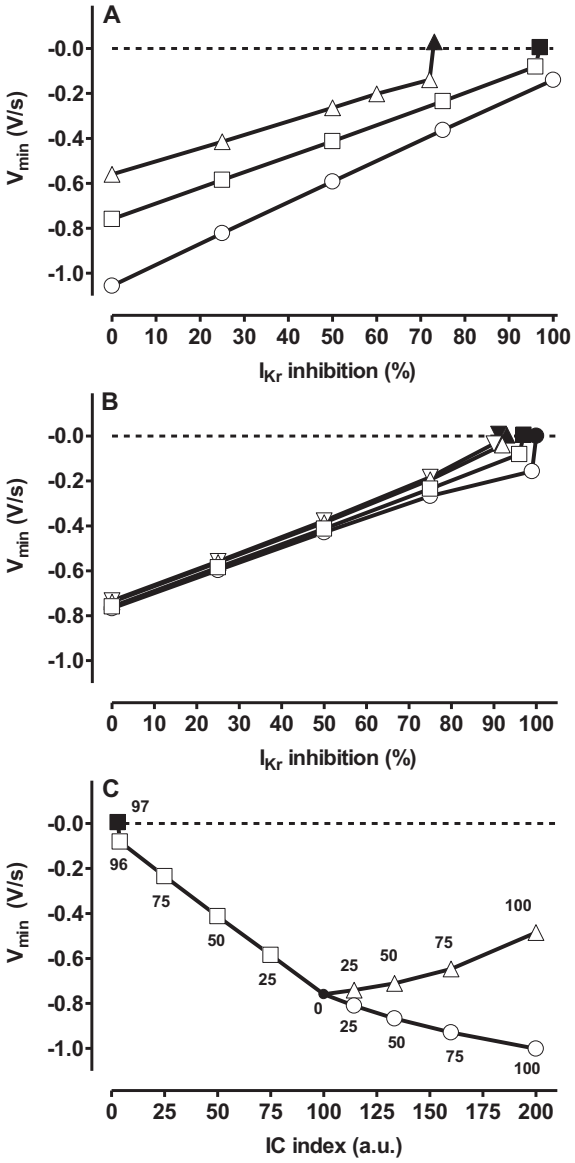

Fig. 2. V_{min} calculated from APs obtained by *in silico* simulation of the human ventricular myocytes using the Dutta revised ORd algorithm with a cycle length of 1000 ms. Panel A shows the difference among epicardial (circles), endocardial (squares) and midmyocardial (triangles) myocytes in the presence of various levels of I_{Kr} inhibition. Panel B shows the effect of various cycle lengths (800 ms, circles; 1000 ms, squares; 2000 ms, triangles and 3000 ms, inverse triangles) in the presence of various levels of I_{Kr} inhibition. Panel C shows the effect of various levels of I_{Kr} (squares), I_{CaL} (triangles) or I_{NaL} (circles) inhibition. The ordinate is the minimal rate of voltage decrease measured at the EAD take-off voltage (V_{min}) expressed as volts per second (V/s). The abscissa is the percentage (%) of inhibition of the I_{Kr} cardiac current (A and B) or the calculated IC index (C). Open and closed symbols represent the absence or presence of EAD. Numbers represent the % of inhibition separately applied on each current. Dotted line represents EAD threshold.

shift of the IC index (< 100) (Fig. 2C). Conversely, an I_{CaL} inhibition increase induced only a slight increase of V_{min} (−0.485 V/s observed at 100% I_{CaL} inhibition) with a rightward shift of the IC index (> 100) while an I_{NaL} inhibition increase induced a V_{min} decrease (−1.001 V/s observed at 100% I_{NaL} inhibition) with a rightward shift of the IC index (> 100) (Fig. 2C).

Various cardiac risk factors such as cardiac pause, hypertrophic cardiomyopathy (HCM), congestive heart failure (CHF), long QT syndrome of type 1, 2 or 3 (LQT1, LQT2, LQT3), hypokalemia and ischemia were tested in order to observe their influence on the incidence of proarrhythmic events on the AP obtained by *in silico* simulation of the human ventricular endocardial myocytes under a CL of 1000 ms using the Dutta revised ORd algorithm. In absence of any I_{Kr} inhibition, the effects of these various cardiac risk factors on the timeline of the AP were illustrated by Fig. 3 (left panels). Ischemia was the only cardiac risk factor shifting the AP to the left resulting in a decrease of all the AP parameters values (Table 1). RMP was not modified by a 2 s pause, HCM, CHF, LQT1, LQT2 or LQT3 conditions but was increased by hypokalemia conditions and decreased by ischemia conditions (Table 1). APA was not modified by 2 s pause, CHF, LQT1 or LQT2 conditions but was increased by HCM, LQT3 and hypokalemia conditions and decreased by ischemia conditions (Table 1). V_{max} was not modified by HCM and LQT1 conditions while V_{max} was increased by 2 s pause and LQT2 conditions and decreased by CHF, LQT3 hypokalemia and ischemia conditions (Table 1). APD_{40}, APD_{60}, APD_{90} and $T_{90–40}$ were increased by all the cardiac risk factors except ischemia (ranked as follows: 2 s pause, LQT1, hypokalemia, LQT2, HCM, CHF and LQT3 from the smallest to the highest effects, respectively) (Table 1). $T_{90–60}$ was decreased by 2 s pause and LQT1 conditions and increased by the other cardiac risk factors except ischemia (ranked as follows: hypokalemia, LQT2, LQT3, CHF, HCM from the smallest to the highest effects,

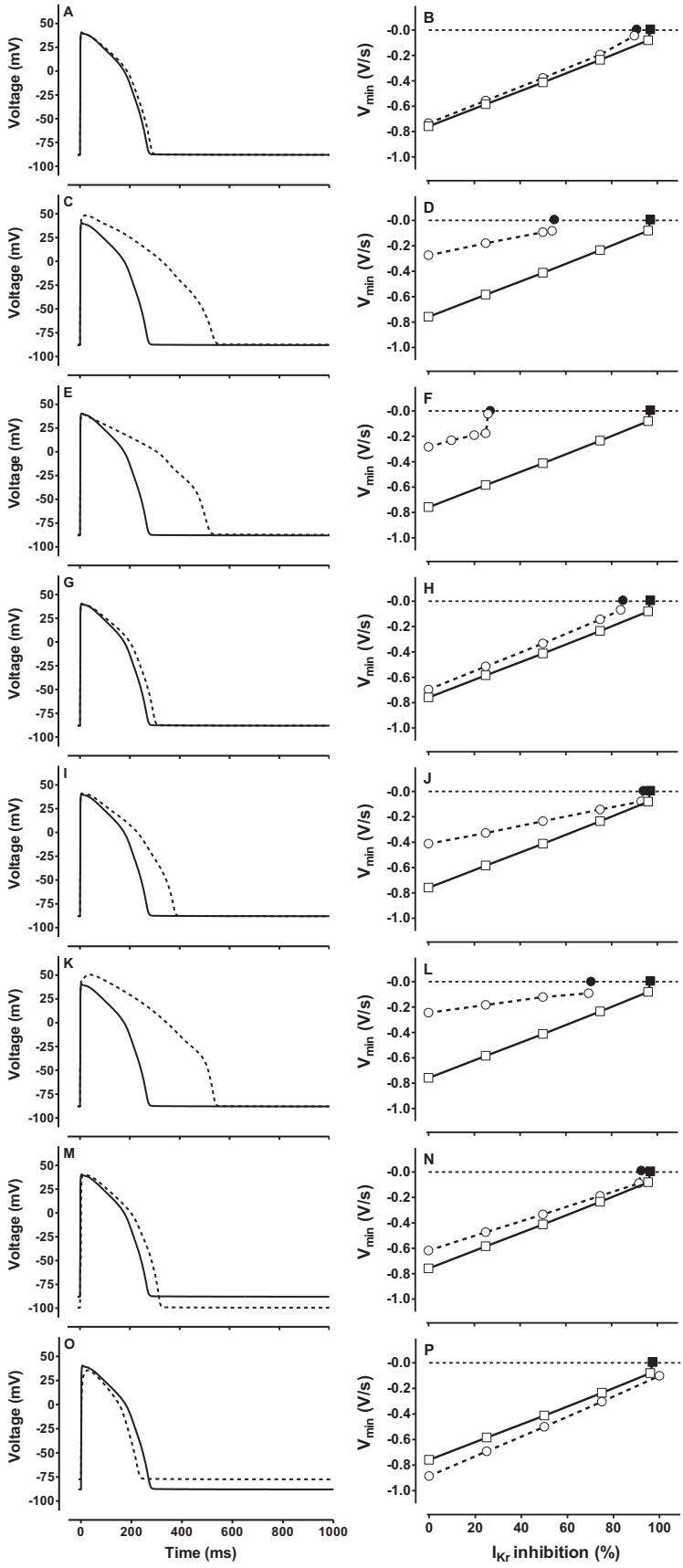

Fig. 3. (Left panels) APs obtained by *in silico* simulation of the human ventricular endocardial myocytes using the Dutta revised ORd algorithm under various experimental conditions with a cycle length of 1000 ms in absence of any cardiac current inhibition (full and dotted line for absence or presence of cardiac risk factor, respectively). The ordinate is the membrane voltage expressed as millivolts (mV). The abscissa is the time expressed as milliseconds (ms). (Right panels) V_{min} calculated from APs obtained by *in silico* simulation of the human ventricular endocardial myocytes using the Dutta revised ORd algorithm with a cycle length of 1000 ms under absence or presence of cardiac risk factor and increasing I_{Kr} inhibition. The ordinate is the minimal rate of voltage decrease measured at the EAD take-off voltage (V_{min}) expressed as volts per second (V/s). The abscissa is the percentage (%) of I_{Kr} inhibition. Open and closed symbols represent the absence or presence of EAD, respectively. Full and dotted lines represent the absence or the presence of a cardiac risk factor, respectively. Horizontal dotted line represents EAD threshold. Cardiac risk factors are the following: 2 s pause (A and B), HCM (C and D), CHF (E and F), LQT1 (G and H), LQT2 (I and J), LQT3 (K and L), hypokalemia (M and N) and ischemia (O and P).

respectively) (Table 1). In the presence of an increasing level of I_{Kr} inhibition, the effects of the various cardiac risk factors on V_{min} were illustrated by Fig. 3 (right panels). The more the I_{Kr} inhibition increased, the more V_{min} increased, V_{min} being equal to zero when EAD was observed. Depending on the risk factor, EAD was observed at various level of I_{Kr} inhibition (27, 55, 71, 85, 91, 93 and 94% for CHF, HCM, LQT3, LQT1, 2 s pause, hypokalemia and LQT2, respectively). In absence of any I_{Kr} inhibition, V_{min} was increased by all the cardiac risk factors except ischemia (ranked as follows: 2 s pause, LQT1, hypokalemia, LQT2, HCM, CHF and LQT3 from the smallest to the highest effects, respectively) (Table 1).

In terms of IC index at which EAD was induced, the various experimental conditions were ranked as follows: non-failing, LQT2, hypokalemia, bradycardia, 2 s pause, LQT1, LQT3, HCM and CHF (IC index of 3, 6, 7, 7 to 9, 9, 15, 29, 45 and 73, respectively). No EAD was observed under ischemic conditions.

3.2. Effects of compounds on EAD occurrence

The effects of 30 compounds were tested under four experimental conditions (non-failing, 2 s pause, HCM and CHF) in order to observe their propensity to induce EAD in a range of 1 to 100-fold their $EFTPC_{max}/IC_{50s}$ ratio. The multiple of $EFTPC_{max}/IC_{50s}$ ratio, the IC index and the V_{min} value at which each compound induced EAD are given in Table 2. Only two compounds (cisapride and quinidine) induced EAD under the four experimental conditions. Three compounds (dofetilide, nilotinib and sotalol) induced EAD under three experimental conditions (2 s pause, HCM and CHF). Twelve compounds (bepridil, chloroquine, chlorpromazine, cibenzoline, flecainide, lopinavir, moxifloxacin, ondansetron, quinine, ranolazine, sertindole and terfenadine) induced EAD only under HCM and CHF conditions. Mibefradil and propafenone induced EAD only under CHF conditions. Finally, nine compounds failed to induce any EAD even at an $EFTPC_{max}/IC_{50s}$ ratio of 100: amiodarone, amitriptyline, azithromycin, diltiazem, lidocaine, mexiletine, ritonavir, rufinamide, saquinavir, toremefine and verapamil.

The IC index and the V_{min} value calculated for each multiple of $EFTPC_{max}/IC_{50s}$ ratio made it possible to establish a profile for each studied compound in order to predict its propensity to induce EAD under various experimental conditions depending on their inhibitory properties of the various cardiac currents. Compounds inducing both a V_{min} increase and a leftward shift of the IC index mainly inhibited outward currents and had a propensity towards EAD occurrence observed at a V_{min} value near to zero and at an IC index which was determined by the experimental conditions. Conversely, compounds inducing a V_{min} decrease and a rightward shift of the IC index never displayed EADs, due to their preferential inhibition of inward currents. As examples, the profiles of six compounds are reported in Fig. 4. Cisapride and dofetilide (mainly inhibiting I_{Kr}) induced a V_{min} increase with an IC index leftward shift. EAD was observed only when the multiple of $EFTPC_{max}/IC_{50s}$ ratio is high enough to allow V_{min} to reach the zero value at the IC index specific for the used experimental conditions (Fig. 4A and B for cisapride and dofetilide, respectively). Lidocaine (mainly inhibiting I_{NaL}) induced a V_{min} decrease and an IC index rightward shift without any propensity to EAD occurrence (Fig. 4C). Mexiletine (mainly inhibiting I_{CaL} and I_{NaL}) induced a V_{min} decrease and an IC index rightward shift without any propensity to EAD occurrence (Fig. 4D). Ritonavir (mainly inhibiting I_{Kr}, I_{CaL} and I_{NaL}) induced a V_{min} increase with an IC index leftward shift without any EAD induction as V_{min} never reached the zero value (Fig. 4E). Finally, verapamil (mainly inhibiting both I_{Kr} and I_{CaL}) showed a dual profile: an increase of V_{min} (not high enough to observe EAD) linked to a mixed right- and leftward shift of the IC index (Fig. 4F).

The relationship between IC index and V_{min} also allowed compound

Table 2
Ability of compounds to induce EAD calculated using the Dutta revised ORd algorithm in human ventricular endocardial myocytes under four experimental conditions and a cycle length of 1000 ms.

	x-fold $EFTPC_{max}/IC_{50s}$ ratio EAD threshold				IC index EAD threshold (a.u)				V_{min} EAD threshold (V/s)			
	NF	P	HCM	CHF	NF	P	HCM	CHF	NF	P	HCM	CHF
Amiodarone	–	–	–	–	–	–	–	–	–	–	–	–
Amitryptiline	–	–	–	–	–	–	–	–	–	–	–	–
Azithromycin	–	–	–	–	–	–	–	–	–	–	–	–
Bepridil	–	–	9	2	–	–	41.5	72.1	–	–	−0.081	−0.161
Chloroquine	–	–	39	6	–	–	49	72.5	–	–	−0.085	−0.171
Chlorpromazine	–	–	89	23	–	–	45	68	–	–	−0.080	−0.157
Cibenzolide	–	–	5	1.3	–	–	44	72.1	–	–	−0.092	−0.166
Cisapride	59	27	5.4	2.1	3.5	9.1	44.9	73.6	−0.070	−0.034	−0.084	−0.163
Diltiazem	–	–	–	–	–	–	–	–	–	–	–	–
Dofetilide	–	21	0.07	0.09	–	9.3	44.2	73.1	–	−0.030	−0.090	−0.158
Flecainide	–	–	1.4	0.4	–	–	45.3	68.8	–	–	−0.086	−0.190
Lidocaine	–	–	–	–	–	–	–	–	–	–	–	–
Lopinavir	–	–	17	4	–	–	34.2	73.1	–	–	−0.070	−0.055
Mexiletine	–	–	–	–	–	–	–	–	–	–	–	–
Mibefradil	–	–	–	14	–	–	–	72.5	–	–	–	−0.111
Moxifloxacin	–	–	28	5	–	–	54	74.2	–	–	−0.082	−0.179
Nilotinib	–	34	2	0.5	–	8.5	44.4	70.8	–	−0.034	−0.086	−0.178
Ondansetron	–	–	7	1.9	–	–	42.9	72	–	–	−0.084	−0.135
Propafenone	–	–	–	1.9	–	–	–	71.3	–	–	–	−0.153
Quinidine	11	5	0.6	0.15	6	9.9	41.9	73.8	−0.086	−0.044	−0.084	−0.208
Quinine	–	–	3.3	2.1	–	–	49	59.3	–	–	−0.072	−0.165
Ranolazine	–	–	8	17	–	–	49.1	35.1	–	–	−0.097	−0.147
Ritonavir	–	–	–	–	–	–	–	–	–	–	–	–
Rufinamide	–	–	–	–	–	–	–	–	–	–	–	–
Saquinavir	–	–	–	–	–	–	–	–	–	–	–	–
Sertindole	–	–	9	1.9	–	–	44.6	73.7	–	–	−0.092	−0.178
Sotalol	–	82	8	1.9	–	9.4	43.6	73.6	–	−0.020	−0.086	−0.185
Terfenadine	–	–	4	0.5	–	–	43.1	71.4	–	–	−0.089	−0.121
Toremefine	–	–	–	–	–	–	–	–	–	–	–	–
Verapamil	–	–	–	–	–	–	–	–	–	–	–	–

a.u., arbitrary unit; V/s, volt/s; NF, non-failing control condition; P, 2 s pause; HCM, hypertrophic cardiomyopathy; CHF, congestive heart failure; –, absence of EAD.

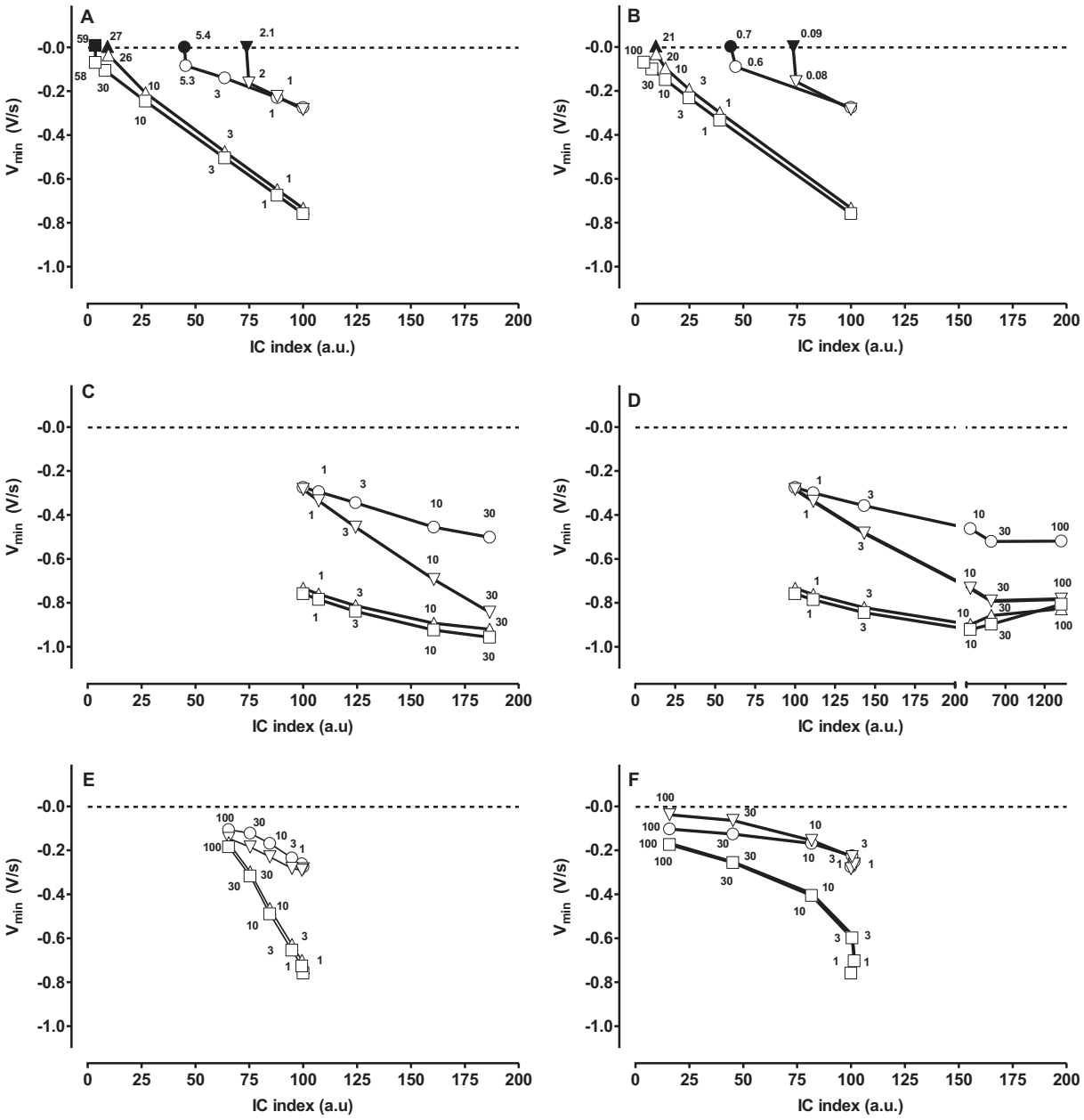

Fig. 4. Relationship between IC index (abscissa, expressed as arbitrary unit, a.u.) and V_{min} (ordinate, expressed as volts/s, V/s) calculated for cisapride (A), dofetilide (B), lidocaine (C), mexiletine (D), ritonavir (E) and verapamil (F) under non-failing (squares), 2 s pause (triangles), HCM (circles) and CHF (inverse triangles) conditions from *in silico* simulation of the human ventricular endocardial myocytes using the Dutta revised ORd algorithm with a cycle length of 1000 ms. Numbers represent the tested multiple of $EFTPC_{max}/IC_{50s}$ ratio. Dotted line represents EAD threshold. Open and closed symbols represent the absence or presence of EAD.

classification into torsadogenic or non-torsadogenic classes. All the compounds inducing EAD had a similar profile: both a V_{min} increase and an IC index leftward shift up to a threshold at which EAD was induced (Fig. 5A, C, E and G for non failing, 2 s pause, HCM and CHF conditions, respectively). Conversely, the profiles observed with compounds which did not induce EAD were highly variable: IC index increase and/or decrease coupled to V_{min} increase or decrease (Fig. 5B, D, F and H for non failing, 2 s pause, HCM and CHF conditions, respectively). This allowed quantification of the threshold necessary to induce an EAD under each experimental condition. The threshold value was calculated to be a V_{min} of -0.078 V/s with an IC index of 4.8 ($n = 2$) under non-failing conditions, a V_{min} of -0.032 ± 0.008 V/s with an IC index of 9.3 ± 0.5 ($n = 5$) under 2 s pause conditions, a V_{min} of -0.084 ± 0.006 V/s with an IC index of 44.8 ± 4.2 ($n = 17$) under HCM conditions, and a V_{min} of -0.157 ± 0.034 V/s with an IC index of 69.5 ± 9.0 ($n = 19$) under CHF conditions (see Table 2). Regarding the propensity of EAD occurrence, the models can be ranked as follows: non-failing < 2 s pause < HCM < CHF. Non-failing experimental conditions required a higher outward current inhibition ratio (*vs.* inward current) to elicit EAD compared to the other conditions. Only compounds such as cisapride and quinidine are able to reach an IC index high enough to induce EAD under the four experimental tested conditions.

Regarding torsadogenicity, all the 8 compounds reported as TdP positive by the WP classification (class 1: bepridil, chlorpromazine, cisapride, dofetilide, quinidine, quinine, sotalol and terfenadine) showed EAD under at least two out of the four tested experimental conditions (see Table 3). Except cibenzoline, all the compounds reported as TdP negative by the WP classification (class 3: diltiazem, lidocaine and verapamil) showed no EAD under the four tested

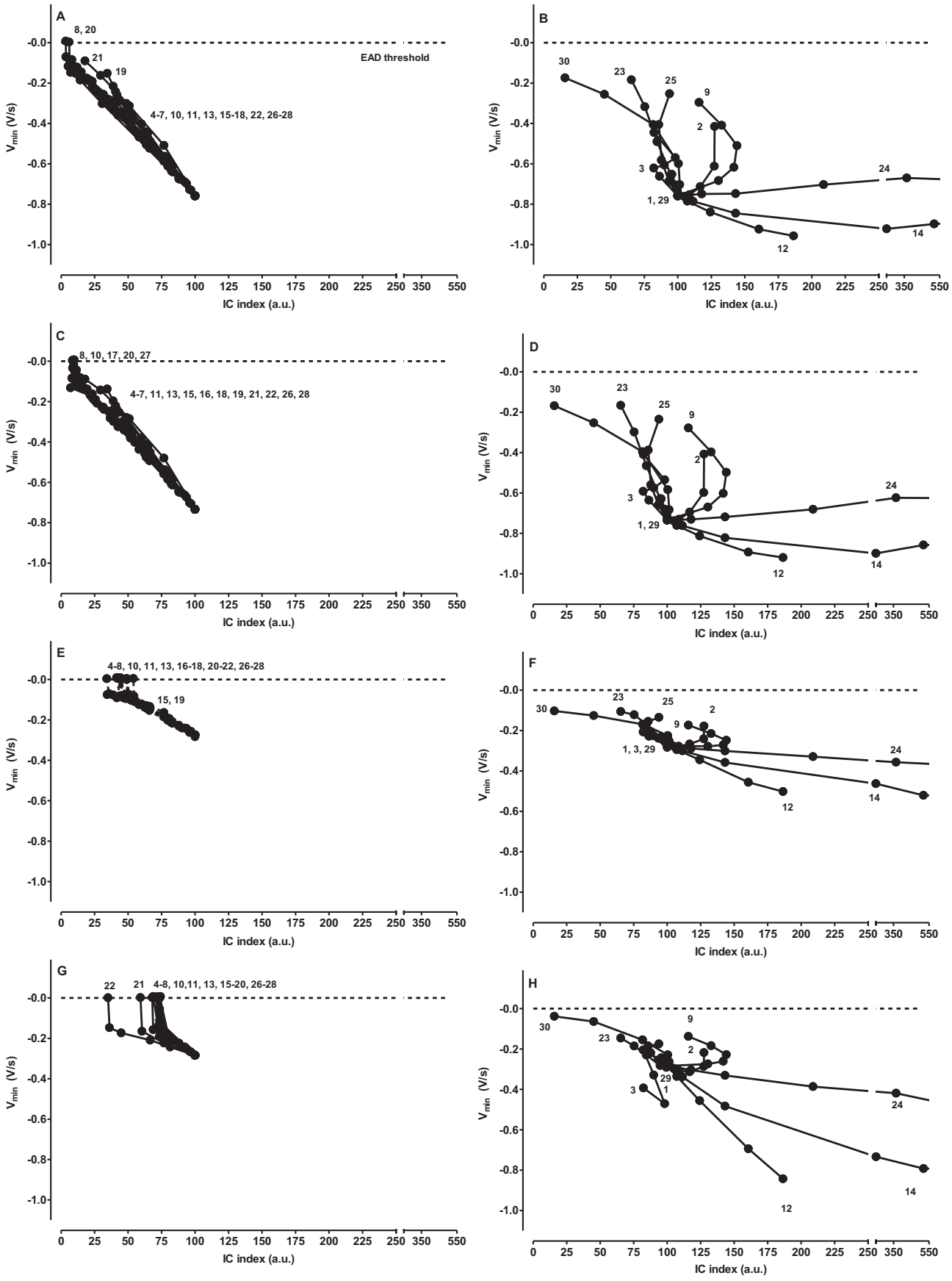

(caption on next page)

Fig. 5. Relationship between IC index (abscissa expressed as arbitrary unit, a.u.) and V_{min} (ordinate expressed as volts/s, V/s) calculated using the Dutta revised ORd algorithm in human ventricular endocardial myocytes with a CL of 1000 ms for compounds inducing TdP (left panels) under at least one of the four tested experimental conditions (A, C, E and G for non-failing, 2 s pause, HCM and CHF, respectively) and compounds inducing no TdP (right panels) whatever the experimental conditions (B, D, F and H for non-failing, 2 s pause, HCM and CHF, respectively). Numbers represent the compounds as follows: amiodarone (1), amytryptiline (2), azithromycin (3), bepridil (4), chloroquine (5), chlorpromazine (6), cibenzoline (7), cisapride (8), diltiazem (9), dofetilide (10), flecainide (11), lidocaine (12), lopinavir (13), mexiletine (14), mibefradil (15), moxifloxacin (16), nilotinib (17), ondansetron (18), propafenone (19), quinidine (20), quinine (21), ranolazine (22), ritonavir (23), rufinamide (24), saquinavir (25), sertindole (26), sotalol (27), terfenadine (28), toremefine (29), verapamil (30). Dotted line represents EAD threshold.

Table 3
Relationship between the TdP risk classification of Wisniowska and Polak (2017) and the presence or absence of EAD under the four tested experimental conditions.

Compound	TdP + /TdP −	Ratio	EAD			
			NF	P	HCM	CHF
Class 1						
Bepridil	15/0	1	−	−	+	+
Chlorpromazine	11/0	1	−	−	+	+
Cisapride	16/0	1	+	+	+	+
Dofetilide	16/0	1	−	+	+	+
Quinidine	16/0	1	+	+	+	+
Quinine	16/0	1	−	−	+	+
Sotalol	14/0	1	−	+	+	+
Terfenadine	16/0	1	−	−	+	+
Class 2						
Amiodarone	11/2	0.85	−	−	−	−
Amitryptiline	5/3	0.65	−	−	−	−
Azithromicyn	5/1	0.83	−	−	−	−
Chloroquine	3/3	0.5	−	−	+	+
Flecainide	8/1	0.89	−	−	+	+
Mexiletine	1/5	0.17	−	−	−	−
Mibefradil	3/4	0.43	−	−	−	+
Moxifloxacin	8/4	0.67	−	−	+	+
Nilotinib	3/1	0.75	−	+	+	+
Ondansetron	4/1	0.8	−	−	+	+
Propafenone	5/4	0.56	−	−	−	+
Ranolazine	2/5	0.28	−	−	+	+
Ritonavir	1/1	0.5	−	−	−	−
Saquinavir	1/4	0.2	−	−	−	−
Sertindole	11/1	0.92	−	−	+	+
Class 3						
Cibenzoline	0/4	0	−	−	+	+
Diltiazem	0/9	0	−	−	−	−
Lidocaine	0/1	0	−	−	−	−
Verapamil	0/13	0	−	−	−	−
Class 4						
Lopinavir	NR	NR	−	−	+	+
Rufinamide	NR	NR	−	−	−	−
Toremefine	NR	NR	−	−	−	−

Class 1, compounds reported as torsadogenic (TdP +) in all the studies; class 2, compounds reported as torsadogenic and non-torsadogenic (TdP + /TdP −) depending on the studies; class 3, compounds reported as non torsadogenic (TdP −) in all the studies; class 4, compounds not reported (NR); Ratio is the number of studies reporting the compound as torsadogenic *vs.* the total number of studies; +, presence of EAD; −, absence of EAD; NF, non-failing; P, 2 s pause; HCM, hypertrophic cardiomyopathy; CHF, congestive heart failure.

experimental conditions. Contingency tables showed a high sensitivity and accuracy of the prediction of compound torsadogenicity, especially under HCM and CHF conditions *vs.* non-failing conditions (Table 4). Six compounds out of 15 reported with a WP contradicting classification (class 2: amiodarone, amitriptyline, azithromycin, mexiletine, ritonavir and saquinavir) were unable to induce EAD when the other compounds (class 2: chloroquine, flecainide, mexiletine, mibefradil, moxifloxacin, nilotinib, ondansetron, propafenone, ranolazine, ritonavir, saquinavir and sertindole) induced EAD at least in 1 of our tested experimental conditions (Table 3). In this case, contingency tables showed a lower sensitivity and accuracy of the prediction of compound torsadogenicity, even if the sensitivity and accuracy of the prediction of compound torsadogenicity remains better under HCM and CHF conditions *vs.* non-failing conditions (Table 4).

Table 4
Contingency tables for Dutta revised ORd model prediction based on the occurrence of EAD observed under four different experimental conditions and the WP torsadogenic risk classification taking into account (i) only uncontroversial classes 1 and 3 or (ii) uncontroversial classes 1 and 3 and controversial class 2.

	TP	FP	FN	TN	PPV	NPV	Sens	Spec	Acc
Classes 1 and. 3									
Non-failing	2	0	6	4	100	40	25	100	50
2 s pause	4	0	4	4	100	50	50	100	67
HCM	8	1	0	3	89	100	100	75	92
CHF	8	1	0	3	89	100	100	75	92
Classes 1, 2 and 3									
Non-failing	2	0	17	8	100	32	11	100	37
2 s pause	5	0	14	8	100	36	26	100	48
HCM	14	2	5	6	88	55	74	75	74
CHF	15	3	4	5	83	56	79	63	74

TP, true positive; FP, false positive; FN, false negative; TN, true negative; PPV, positive predictive value; NPV, negative predictive value; Sens, sensitivity; Spec, specificity; Acc, accuracy; HCM, hypertrophic cardiomyopathy; CHF, congestive heart failure. TP, FP, FN and TN are expressed as number of observations. PPV, NPV, Sens, Spec and Acc are expressed as percentage (%).

4. Discussion

The present study characterized 30 drugs with various degrees of torsadogenic risk for their ability to induce EADs using *in silico* simulations of the human ventricular action potential. The use of *in silico* action potential simulations is one of the pillars of the CiPA paradigm (Sager et al., 2014). We examined the 30 drugs in simulations of healthy and various cardiac risk factor settings, in order to provide a more complete profile of drug-induced torsadogenic risk. As indicated in Fig. 4 and Table 2, in healthy, non-failing simulations, EADs were rarely observed, even for drugs classified as torsadogenic, and only at high multiples of the free plasma C_{max}. In contrast, under conditions simulating either CHF or HCM, EADs for drugs classified as torsadogenic were observed at concentrations much closer to therapeutic C_{max}. These findings support the notion that drug-induced torsade is a rare event and likely requires underlying cardiac risk factors to be present. As an example, dofetilide is categorized as a drug with a “high” torsadogenic risk according to the CiPA risk assignment. However, in a dofetilide clinical study in healthy volunteers, although associated with large (≈80 ms) increases in QTc interval no arrhythmias were observed (Le Coz, Funck-Brentano, Morell, Ghadanfar, & Jaillon, 1995). In patients prescribed dofetilide for supraventricular arrhythmias, the incidence of TdP has been reported to be 0.8% (Pritchett & Wilkinson, 1999). Interestingly, in patients with CHF, the incidence of dofetilide-related TdP increased to 3.3% (Torp-Pedersen et al., 1999). The results from the present study are consistent with these clinical findings. Under conditions simulating a non-failing, healthy human ventricular action potential, dofetilide is not associated with EADs even at multiples much higher than therapeutic. However, in the context of cardiac risk factors such as CHF and HCM, EADs occur very near the therapeutic Cmax, confirming our preliminary results (Crumb et al., 2017). As another example, cisapride is listed as an “intermediate” TdP risk drug according to CiPA risk assignment. Cisapride was a widely prescribed drug with over 140 million patient treatments (Markiewicz and Vanden

Plas, 2000) and 34 reports of TdP (Wysowski & Bacsanyi, 1996). Approximately 39% of those patients developing TdP had underlying cardiac risk factors. The data shown here support the rare occurrence of cisapride-related TdP since only under conditions which simulate CHF or HCM were EADs observed at near therapeutic concentrations. EADs were observed at 2 to 5-fold C_{max} under these simulated conditions. Interestingly, 56% of the patients which developed TdP were taking drugs which inhibited cisapride metabolism leading to higher than anticipated plasma concentrations (Wysowski, Corken, Gallo-Torres, Tlarico, & Rodriguez, 2001). Mexiletine, a sodium channel blocking antiarrhythmic, and verapamil, a calcium channel blocking antihypertensive, are listed as having "no" risk of TdP. At no concentration and under no simulated conditions did these drugs elicit EADs, consistent with their clinical profiles.

Finding a metric allowing more accurate quantitative preclinical detection of proarrhythmic liabilities of new drug candidates remains the goal of the CiPA initiative. The present study demonstrated that the relationship existing between IC index and V_{min} allowed quantitative determination of the threshold at which a compound induced an EAD under various experimental conditions. An IC index lower than 100 coupled to a V_{min} value near to zero indicated a risk of EAD as an all or none phenomena obtained at a threshold which was dependent upon the simulated clinical situation. Drugs could be identified as non torsadogenic under non-failing conditions and as torsadogenic under pathological conditions depending on their ability to reach a defined level of IC index linked to the impact of pre-existing cardiovascular pathological situations. This was the case with selective I_{Kr} blockers (cisapride, dofetilide, sertindole) or drugs which blocked I_{Kr} more than I_{CaL} and/or I_{NaL} (bepridil, chloroquine, chlorpromazine, cibenzoline, flecainide, lopinavir, mibefradil, moxifloxacin, nilotinib, ondansetron, propafenone, quinidine, quinine, ranolazine, sotalol and terfenadine). A right- and/or leftward shift of the IC index coupled to a low V_{min} increase (not high enough to reach zero value) indicated no risk of EAD whatever the experimental conditions. This was the case with drugs which block I_{Kr}, I_{CaL} and/or I_{NaL} (amiodarone, amitryptiline, azithromycin, diltiazem, ritonavir, saquinavir and verapamil). A rightward shift of the IC index coupled to a V_{min} decrease indicated no risk of EAD whatever the experimental conditions. This was the case with drugs which block I_{CaL} and/or I_{NaL} (lidocaine, mexiletine and rufinamide).

Are the present results consistent with the TdP risk classification of compounds? Taking into account only uncontroversial classes of the WP classification, contingency tables showed a higher sensitivity and accuracy of the predictability of compound torsadogenicity under failing conditions, especially HCM and CHF. All the eight tested compounds from WP class 1 classification (TdP positive) showed EAD under at least two of our tested experimental conditions (HCM and CHF) whereas three out of four tested compounds from the class 3 classification (TdP negative) showed no EAD whatever the experimental conditions, suggesting a high accuracy of the present results with the WP TdP risk classification, especially in the presence underlying cardiac risk factors. The only one misclassified compound from class 3 was cibenzoline which showed EAD only under HCM or CHF conditions, confirming EAD induction observed under pathological situation such as multifocal ventricular arrhythmias in the dog for example (Dangman, 1984) or the increased QTc interval and the increased number of patients with "break-through" arrhythmias on chronic cibenzoline therapy described by Miura et al. (1985). In a recent *in silico* study (McMillan et al., 2017), cibenzoline was classified as non torsadogenic using an I_{CaL} increase EAD metric and as torsadogenic using APD_{90} or hERG IC_{50}/$EFTPC_{max}$ metrics. A difference in the species used for patch clamp data is to be mentioned between this study (animals/human) and the present results (only human). This discrepancy regarding cibenzoline remained to be studied in more details in order to understand this misclassification of the compound. The WP classification also reported a contradictory torsadogenic risk for compounds of class 2 (both TdP positive and TdP negative depending on the studies). In this case, contingency tables also showed a higher sensitivity and accuracy of the predictability of compound torsadogenicity under failing conditions, especially HCM and CHF. Nevertheless, taking into account this contradictory class 2 of compounds decreased the sensitivity and accuracy of predictability of compound torsadogenicity (see Table 4). Once again, this highlight the difficulty to estimate the accuracy of a preclinical TdP metric when the compound classification into TdP risk categories based on their clinical behaviour remains a very difficult problem due to the very high variability of human clinical situation (Wisniowska & Polak, 2017, McMillan et al., 2017, Mason, 2017). In the WP classification, if we consider as torsadogenic compounds with a TdP positive/TdP negative ratio higher than 50% (Table 3), 10 compounds out of 15 were correctly classified. Chloroquine, flecainide, moxifloxacine, nilotinib, ondansetron, propafenone and sertindole were identified as torsadogenic compounds at least under conditions which simulate CHF or HCM. Mexiletine, ritonavir and saquinavir were identified as non torsadogenic compounds even under conditions which simulate CHF or HCM. Three compounds were misclassified as "false negative" (amiodarone, amitryptiline and azithromycin) and two compounds as "false positive" (mibefradil and ranolazine). Nevertheless, the TdP risk classification of these compounds is still ambiguous. Amiodarone could be a candidate for re-classification into a less TdP risk category due to its small effect on various metrics based on increase in APD or decreased EAD thresholds as already suggested by McMillan et al. (2017) and/or its very low incidence of proarrhythmic complication as discussed by Schrickel et al., (2006). Cardiovascular safety of azithromycin and amitryptiline seems to be still inconclusive and could also be linked to pre-existing risk factor such as bradycardia, hypokalemia, hypomagnesemia, use of high dose, impaired elimination and/or concomitant use of QT drug (Lu et al., 2014; Lubna et al., 2017). The same observation could be made for mibefradil which was withdrawn from the market after several dangerous interactions with at least 25 drugs and the bradycardia associated to its hypotensive effect (Riley, Witton, & Shakir, 2002). TdP risk classification of ranolazine remained also controversial: on the one hand, a very low TdP risk is reported by CiPA (Fermini et al., 2015) and on the other hand, conditional TdP risk linked to hypokalemia, hypomagnesemia, use of high dose, impaired elimination and/or concomitant use of QT drug is reported by Crediblemeds (Woosley et al., 2018).

Prediction of an unacceptable risk of TdP remains a major goal of cardiac safety pharmacology. It is now recognised that QT prolongation is an imperfect surrogate marker for risk of TdP, (see Hondeghem, 2008, 2018 for review). In line with the CiPA initiative, various *in silico* parameters were proposed to help this prediction (see Parikh, Gurev, & Rice, 2017 for review). The present results were based on the determination of an IC index – V_{min} metric. As the IC index is a property specific to each compound and V_{min} is a property specific to each experimental condition, this IC index – V_{min} metric allowed to quantify at which threshold a compound induced an EAD under healthy or mimicked disease state conditions from APs obtained by *in silico* simulation of the human ventricular endocardial myocytes using the Dutta revised ORd algorithm. This simulation study was performed by changing channels conductances based on IC_{50s} reported by Crumb et al. (2016). Taking into account binding kinetics (as explored by recent studies regarding only I_{Kr} channel, see Dutta et al., 2016, Dutta, Chang, et al., 2017) is certainly also to consider in order to improve cardiac safety profile prediction. This simulation study was also performed only at the cellular level even if it is important to take into account the organ/body level as cell to cell coupling, tissue synchronisation, propagation of EAD across the whole heart, fibrosis, myocytes death, parameters which are also of major importance in order to understand the real picture of the clinical situation (see Zemzemi et al., 2013 for discussion). This more integrated level of investigations is also to be considered in order to improve TdP risk prediction in susceptible patient. Even if mathematical algorithm still requires refinement in order to better reflect the biological/clinical reality, it could be a step in the

comprehension of the mechanism as this model of AP simulation is able to reproduce EAD within the human situation and is now recognised as a useful model by the CiPA initiative. Even if the mechanistic understanding remains incomplete, the choice of EAD as marker (Christophe, 2013, McMillan et al., 2017) remains interesting due to its implication as primary mechanism promoting arrhythmias in acquired and congenital LQT syndromes including TdP, polymorphic ventricular tachycardia or ventricular fibrillation (see Weiss, Garfinkel, Karagueuzian, Cheng, & Qu, 2010 for review). EAD is a secondary voltage depolarization occurring in a fixed voltage range during the AP repolarization phase: if the repolarization rate is too slow within this voltage window, calcium current can grow larger than potassium current and reverse repolarization to cause an EAD (Weiss et al., 2010 and Qu et al., 2013, for mechanism review). In consequence, this EAD take-off membrane voltage offers a stable reference linked to a critical phase of the EAD upstroke. Moreover, under our various experimental conditions, the minimal rate of AP voltage decrease at this EAD take-off membrane voltage (V_{min}) showed a sign inversion at the EAD take-off voltage observed at a voltage ranked from −17 to −23 mV, in agreement with the −22 mV experimentally observed in human isolated endomyocytes (Guo et al., 2011) or in human-induced pluripotent stem cell-derived cardiomyocytes (Ma et al., 2011). The IC index was calculated as the ratio of the potency of a compound to inhibit important inward (I_{CaL} and I_{NaL}) and outward (I_{Kr}) cardiac currents. However, I_{Kr}, I_{CaL} and I_{NCX} are among the most important inward and outward cardiac currents involved in EAD upstroke (see Weiss et al., 2010 for review). The role of another cardiac ionic current such as I_{NaL} was also recently exemplified (Trenor et al., 2012). Inserting I_{NCX} data into the IC index calculation could probably be useful when data on I_{NCX} inhibition data will be available for the various compounds.

Could this IC index – V_{min} metric be considered as a global indicator of the propensity to develop EAD? This metric allowed the quantification of various well known observations such as (i) the higher propensity of midmyocardial cell to develop EAD *vs.* epi- and endo-cardial myocytes (Antzelevitch, 2007), (ii) the higher propensity to develop EAD with lower rate of stimulation (O'Hara et al., 2011) and (iii) the higher propensity to develop EAD in the presence of various underlying cardiac risk factors (Woosley, Heise, Gallo, et al., 2018). The IC index – V_{min} metric classified the various studied models regarding their increasing propensity to develop EAD as follows: ischemia, non-failing, LQT2, hypokalemia, bradycardia, 2 s pause, LQT1, LQT3, HCM and CHF. Is this classification in agreement with the clinical situation? Even if this classification is to be considered as indicative due to the limitations already discussed, some observations are in agreement with the literature. As expected, the present results confirmed that the various tested mimicked clinical situations (with the exception of ischemia) facilitated EAD occurrence: more complex pathological states (such as HCM or CHF) induced EAD at a lower threshold than the various less complex states (such as LQT2, hypokalemia, bradycardia, 2 s pause, LQT1 or LQT3). Misuzawa et al. (2014) reported that LQT3 patients (older than 40 years) had significantly more cumulative lethal arrhythmic events than LQT1, LQT2 or genotype-negative patients. Similarly, Kozhevnikov et al. (2002) reported that underlying cardiac risk factors such as cardiac hypertrophy increased the incidence of TdP. If ischemia is able or not able to induce EAD remained to be studied in more details. No EAD were induced under *in silico* simulation (this study but also Gemmell et al., 2016 or Dutta, Mincholé, et al., 2017). EAD were elicited in only 2 dogs out of 12 (16%) under *in vivo* acute myocardial ischemia without reperfusion (Zhang et al., 2002). No case of TdP was observed in 91 adult patients (placebo group) with ischemic heart disease history (Torp-Pedersen, Camm, Butterfield, Dickinson, & Beatch, 2013).

The present study was focused on the ability of drugs to induce EADs in the absence or presence of various cardiac risk factors. It is also important to keep in mind that cardiac liabilities other than TdP risk (such as negative inotropic effect, arrhythmogenicity not leading to TdP, abnormal depolarization,....) are also to be taken into account in the absence or presence of various cardiac risk factors in order to improve the CiPA initiative. For examples, some calcium channel blocking drugs could be contraindicated in patients with CHF due to their negative inotropic effect on cardiac contractility (Mahé, Chassany, Grenard, Caulin, & Bergmann, 2003) or a sodium channel blocking drug such as pilsicainide induced ventricular arrhythmia and T-wave alternans in patients with Brugada syndrome (Morita et al., 2003).

In conclusion, the present study provided a mechanistic support highlighting the impact of pre-existing cardiovascular disease on arrhythmic events detection suggesting that disease state modelling may need to be incorporated in order to fully realize the goal of the CiPA paradigm in a more accurate predictability of proarrhythmic liabilities of new drug candidate. Furthermore, this study provides a very simple quantitative metric in order to try to better predict TdP risk based on the relationship existing between the potency of a compound to inhibit the most important inward and outward cardiac currents (IC index) and the minimal rate of AP voltage decrease at the EAD take-off voltage (V_{min}). This IC index-V_{min} metric is applicable whatever the experimental model: type of cells, heart rate, external ionic concentrations or changes applied in order to mimic impact of underlying cardiac proarrhythmic risk factors.

Author contributions

BC and WJC conceived the study; BC designed the study, performed the *in silico* drug assays, analysed the data, prepared the tables and figures, BC and WJC interpreted the results, drafted, edited and revised the manuscript.

Conflict of interest

Authors have declared the existence of no conflict of interest.

Funding

This research did not receive any specific grant from funding agencies in the public, commercial, or not-for-profit sector.

Acknowledgements

The authors wish to thank Dr. Rashmi Shah and Dr. Adam Hill for their helpful suggestions and comment.

References

Antzelevitch, C. (2007). Ionic, molecular, and cellular bases of QT-interval prolongation and torsade de pointes. *Europace, 9*(4), iv4–iv15.

Cavero, I., & Holzgrefe, H. (2014). Comprehensive in vitro proarrhythmia assay, a novel in vitro/in silico paradigm to detect ventricular proarrhythmic liability: A visionary 21st century initiative. *Expert Opinion on Drug Safety, 13*(6), 745–758.

Cavero, I., & Holzgrefe, H. (2015). CiPA: Ongoing testing, future qualification procedures and pending issues. *Journal of Pharmacological and Toxicological Methods, 76*, 27–37.

Chang, K. C., Dutta, S., Mirams, G. R., Beattie, K. A., Sheng, J., Tran, P. N., ... Li, Z. (2017). Uncertainty quantification reveals the importance of data variability and experimental design considerations for in silico proarrhythmia risk assessment. *Frontiers in Physiology, 8*, 917.

Christophe, B. (2013). Simulation of early after-depolarisation in non-failing human ventricular myocytes: Can this help cardiac safety pharmacology? *Pharmacological Reports, 65*, 1281–1293.

Christophe, B. (2015). In silico study of transmural dispersion of repolarisation in non-failing human ventricular myocytes: Contribution to cardiac safety pharmacology. *British Journal of Pharmaceutical Research, 7*(2), 88–101.

Crumb, W. J., Christophe, B., & Shah, R. R. (2017). Impact of disease state on arrhythmic event detection using APD modelling. *Journal of Pharmacological and Toxicological Methods, 88*, 205.

Crumb, W. J., Vicente, J., Johannesen, J., & Strauss, D. J. (2016). An evaluation of 30 clinical drugs against the comprehensive in vitro proarrhythmia assay (CiPA) proposed ion channel panel. *Journal of Pharmacological and Toxicological Methods, 81*, 251–262.

Dangman, K. H. (1984). Cardiac effect of cibenzoline. *Journal of Cardiovascular*

Pharmacology, 6(2), 300–311.
Darpo, B. (2010). The thorough QT/QTc study 4 years after the implementation of the ICH E14 guidance. *British Journal of Pharmacology, 159*(1), 49–57.
Dutta, S., Chang, K. C., Beattie, K. A., Sheng, J., Tran, P. N., Wu, M., ... Li, Z. (2017). Optimization of an in silico cardiac cell model for proarrhythmia risk assessment. *Frontiers in Physiology, 8*, 616.
Dutta, S., Mincholé, A., Quinn, T. A., & Rodriguez, B. (2017). Electrophysiological properties of computational human ventricular cell action potential models under acute ischemic conditions. *Progress in Biophysics and Molecular Biology, 129*, 45–52.
Dutta, S., Strauss, D., Colatsky, T., & Li, Z. (2016). Optimization of an in silico cell model for proarrhythmia risk assessment. *Computing in Cardiology, 43*. https://doi.org/10.22489/CinC.2016.253-483.
Fermini, B., Hancox, J. C., Abi-Gerges, N., Bridgland-Taylor, M., Chaudhary, K. W., Colatsky, T., ... Vandenberg, J. I. (2015). A new perspective in the field of cardiac safety testing through the comprehensive in vitro proarrhythmia assay paradigm. *Journal of Biomolecular Screening, 21*(1), 1–11.
Gemmell, P., Burrage, K., Rodriguez, B., & Quinn, T. A. (2016). Rabbit-specific computational modelling of ventricular cell electrophysiology: Using populations of models to explore variability in the response to ischemia. *Progress in Biophysics and Molecular Biology, 121*(2), 169–184.
Guo, D., Liu, Q., Elliot, G., Gingras, M., Kowey, P. R., & Yan, G. X. (2011). Electrophysiological properties of HBI-3000: A new antiarrhythmic agent with multiple-channel blocking properties in human ventricular myocytes. *Journal of Cardiovascular Pharmacology, 57*(1), 79–85.
Hondeghem, L. M. (2008). QT prolongation is an unreliable predictor of ventricular arrhythmia. *Heart Rhythm, 5*(8), 1210–1212.
Hondeghem, L. M. (2018). Drug-induced QT prolongation and torsades de pointes: An all-exclusive relationship or time for an amicable separation? *Drug Safety, 41*(1), 11–17.
Kay, G. N., Plumb, V. J., Arciniegas, J. G., Henthorn, R. W., & Waldo, A. L. (1983). Torsade de pointes: The long-short initiating sequence and other clinical features: Observations in 32 patients. *Journal of the American College of Cardiology, 2*(5), 806–817.
Kleiman, R. B., Shah, R. R., & Morganroth, J. M. (2014). Replacing the thorough QT study: Reflections of a baby in the bath water. *British Journal of Clinical Pharmacology, 78*(2), 195–201.
Kozhevnikov, D. O., Yamamoto, K., Robotis, D., Restivo, M., & El-Sherif, N. (2002). Electrophysiological mechanism of enhanced susceptibility of hypertrophied heart to acquired torsade de pointes arrhythmia: Tridimentional mapping of activation of recovery patterns. *Circulation, 105*(9), 1128–1134.
Le Coz, F., Funck-Brentano, C., Morell, T., Ghadanfar, M. M., & Jaillon, P. (1995). Pharmacokinetic and pharmacodynamic modelling of the effects of oral and intravenous administrations of dofetilide on ventricular repolarisation. *Clinical Pharmacology and Therapeutics, 57*(5), 533–542.
Lu, Z. K., Yuan, J., Li, M., Sutton, S. S., Rao, G. A., Jacob, S., & Bennett, C. (2014). Cardiac risks associated with antibiotics: Azithromycin and levofloxacin. *Expert Opinion on Drug Safety, 14*(2), 295–303.
Lubna, N. J., Wada, T., Nakamura, Y., Chiba, K., Cao, X., Izumi-Nakaseko, H., ... Sugiyama, A. (2017). Amitryptiline may have possibility to induce Brugada syndrome rather than long QT syndrome. *Cardiovascular Toxicology, 18*(1), 91–98.
Ma, J., Guo, L., Fiene, S. J., Anson, B. D., Thomson, J. A., Klamp, T. J., ... January, C. T. (2011). High purity human-induced pluripotent stem cell-derived cardiomyocytes: Electrophysiological properties of action potentials and ionic currents. *The American Journal of Physiology – Heart and Circulatory Physiology, 301*(5), H2006–H2017.
Mahé, I., Chassany, O., Grenard, A. S., Caulin, C., & Bergmann, J. F. (2003). Defining the role of calcium channel antagonists in heart failure due to systolic dysfunction. *American Journal of Cardiovascular Drugs: Drugs, Devices and Other Interventions, 3*(1), 33–41.
Markiewicz, M., & Vanden Plas, Y. (2000). Should cisapride have been “blacklisted”? *Archives of Disease in Childhood. Fetal and Neonatal Edition, 82*(1), F3–F4.
Mason, J. W. (2017). Cardiologist's point of view: Novel ECG biomarkers and in silico models for proarrhythmic risk prediction: Are we ready? *Journal of Electrocardiology, 50*(6), 825–827.
McMillan, B., Gavaghan, D. J., & Mirams, G. R. (2017). Early afterdepolarisation tendency as a simulated pro-arrhythmic risk indicator. *Toxicological Research, 6*(6), 912–921.
Mirams, G. R., Cui, Y., Sher, A., Fink, M., Cooper, J., Heath, B. M., ... Noble, D. (2011). Simulation of multiple ion channel block provides improved early prediction of compounds' clinical torsadogenic risk. *Cardiovascular Research, 91*(1), 53–61.
Mirams, G. R., Davies, M. R., Brough, S. J., Bridgland-Taylor, M., Cui, Y., Gavaghan, D. J., & Abi-Gerges, N. (2014). Prediction of thorough QT study results using action potential simulations based on ion channel screens. *Journal of Pharmacological and Toxicological Methods, 70*(3), 246–254.
Mirams, G. R., & Noble, D. (2011). Is it time for in silico simulation of drug cardiac side effects? *Annals of the New York Academy of Sciences, 1245*, 44–47.
Misuzawa, Y., Horie, M., & Wilde, A. A. (2014). Genetic and clinical advances in congenital long QT syndrome. *Circulation Journal, 78*, 2827–2833.
Miura, D. S., Keren, G., Torres, V., Butler, B., Aogaichi, K., & Somberg, J. C. (1985). Antiarrhythmic effects of cibenzoline. *American Heart Journal, 109*(4), 827–833.
Morita, H., Morita, S. T., Nagase, S., Banba, K., Nishii, N., Tani, Y., ... Ohe, T. (2003). Ventricular arrhythmia induced by sodium channel blocker in patients with Brugada syndrome. *Journal of American College of Cardiology, 42*(9), 1624–1631.
O'Hara, T., Virág, L., Varró, A., & Rudy, Y. (2011). Simulation of the undiseased human cardiac ventricular action potential: Model formulation and experimental validation. *PLoS Computational Biology, 7*(5), e1002061.
Parikh, J., Gurev, V., & Rice, J. J. (2017). Novel two-step classifier for torsades de pointes risk stratification from direct features. *Frontiers in Pharmacology, 8*, 816.
Passini, E., Britton, O. J., Lu, H. R., Rohrbacher, J., Hermans, A. N., Gallacher, D. J., ... Rodriguez, B. (2017). Human in silico drug trials demonstrate higher accuracy than animal models in predicting clinical pro-arrhythmic cardiotoxicity. *Frontiers in Physiology, 8*, 668.
Passini, E., Mincholé, A., Coppini, R., Cerbai, E., Rodriguez, B., Severi, S., & Bueno-Orovio, A. (2016). Mechanisms of pro-arrhythmic abnormalities in ventricular repolarisation and anti-arrhythmic therapies in human hypertrophic cardiomyopathy. *Journal of Molecular and Cellular Cardiology, 96*, 72–81.
Pritchett, E. L., & Wilkinson, W. E. (1999). Effect of dofetilide on survival in patients with supraventricular arrhythmias. *American Heart Journal, 138*(5 Pt 1), 994–997.
Qu, Z., Xie, L.-H., Olcese, R., Karagueuzian, H. S., Cheng, P.-S., Garfinkel, A., & Weiss, J. N. (2013). Early afterdepolarisation in cardiac myocytes: Beyond reduced repolarisation reserve. *Cardiovascular Research, 99*(1), 6–15.
Riley, J., Witton, L. V., & Shakir, S. A. (2002). A post-marketing observational study to assess the safety of mibefradil in the community in England. *International Journal of Clinical Pharmacology and Therapeutics, 40*(6), 241–248.
Rodriguez, B., Trayanova, N., & Noble, D. (2006). Modeling cardiac ischemia. *Annals of the New York Academy of Sciences, 1080*, 395–414.
Sager, P. T., Gintant, G., Turner, J. R., Petit, S., & Stockbridge, N. (2014). Rechanneling the cardiac proarrhythmia safety paradigm: A meeting report from the cardiac safety research consortium. *American Heart Journal, 167*(3), 292–300.
Sarganas, G., Garbe, E., Klimpel, A., Hering, R. C., Bronder, E., & Haverkamp, W. (2014). Epidemiology of symptomatic drug-induced long QT syndrome and torsade de pointes in Germany. *Europace, 16*(1), 101–108.
Schrickel, J. W., Schwab, J. O., Yang, A., Bielik, H., Bitzen, A., Lüderitz, B., & Lewalter, T. (2006). Pro-arrhythmic effects of amiodarone and concomitant rate-control medication. *Europace, 8*(6), 403–407.
Tisdale, J. E. (2016). Drug-induced QT interval prolongation and torsades de pointes: Role of the pharmacist in risk assessment, prevention and management. *Canadian Pharmacists Journal, 149*(3), 139–152.
Torp-Pedersen, C., Camm, A. J., Butterfield, N. N., Dickinson, G., & Beatch, G. N. (2013). Vernakalant: Conversion of atrial fibrillation in patients with ischemic heart disease. *International Journal of Cardiology, 166*(1), 147–151.
Torp-Pedersen, C., Møller, M., Bloch-Thomsen, P. E., Køber, L., Sandøe, E., Egstrup, K., ... Camm, A. J. (1999). Dofetilide in patients with congestive heart failure and left ventricular dysfunction. Danih investigations of arrhythmia and mortality on dofetilide study group. *The New England Journal of Medicine, 341*(12), 857–865.
Trenor, B., Cardona, K., Gomez, J. F., Rajamani, S., Ferrero, J. M., Jr., Belardinelli, L., & Saiz, J. (2012). Simulation and mechanistic investigation of the arrhythmogenic role of the late sodium current in human heart failure. *PLoS One, 7*(3), e32659.
Weiss, J. N., Garfinkel, A., Karagueuzian, H. S., Cheng, P.-S., & Qu, Z. (2010). Early afterdepolarisation and cardiac arrhythmias. *Heart Rhythm, 7*(12), 1891–1899.
Wisniowska, B., & Polak, S. (2017). Am I or Am I not proarrhythmic? Comparison of various classifications of drug TdP propensity. *Drug Discovery Today, 22*, 10–16.
Woosley, R. L., Heise, C. W., Gallo, T., Woosley, R. D., & Romero, K. A.. QTfactors List. (2018). http://www.crediblemeds.org (Accessed 01 May 2018).
Woosley, R. L., Heise, C. W., & Romero, K. A.. QTdrugs List. (2018). http://www.crediblemeds.org (Accessed 01 May 2018).
Wysowski, D. K., & Bacsanyi, J. (1996). Cisapride and fatal arrhythmia. *The New England Journal of Medicine, 335*, 290–291.
Wysowski, D. K., Corken, A., Gallo-Torres, H., Tlarico, L., & Rodriguez, E. M. (2001). Postmarketing reports of QT prolongation and ventricular arrhthymia in association with cisapride and food and drug administration regulatory actions. *The American Journal of Gastroenterology, 96*(6), 1698–1703.
Zemzemi, N., Bernabeu, M. O., Saiz, J., Cooper, J., Pathmanathan, P., Mirams, G. R., ... Rodriguez, B. (2013). Computational assessment of drug-induced effects on the electrocardiogram: From ion channel to body surface potentials. *The British Journal of Pharmacology, 168*, 718–733.
Zhang, C., Xu, D., Li, Y., Liu, N., Zongh, J., ... Lu, Z. (2002). Experimental study of the effect of autonomic nervous system on the transmural dispersion of ventricular repolarisation under acute myocardial ischemia in vivo. *Journal of Huazhong University of Science and Technology, Medical Sciences, 22*(2), 96–99.